Annual Amphidromes: A Common Feature in the Ocean?

Ge Chen

Key Laboratory of Ocean Remote Sensing, Ministry of Education

Ocean Remote Sensing Institute, Ocean University of China, Qingdao

5 Yushan Road, Qingdao 266003, China

Tel & Fax: +86-532-2032424; E-mail: gechen@public.qd.sd.cn

Graham D. Quartly

Laboratory for Satellite Oceanography, National Oceanography Centre, Southampton

Empress Dock, Southampton, Hants, SO14 3ZH, UK

Tel: +44-23-8059-6412; Fax: +44-23-8059-6400; E-mail: gdq@noc.soton.ac.uk

Abstract

The scientific term “amphidrome” is usually associated with tides in oceanography. The dozen tidal amphidromes observed in the ocean are critical points that determine the fundamental pattern of the global tidal system. Exploration of the recently available satellite data with an unprecedented 1-2 decades duration suggests that an amphidrome is not a tide-only phenomenon in the ocean. Analysis of altimeter-derived sea level anomaly (SLA) data and radiometer-derived sea surface temperature (SST) data allows 10 amphidromic points to be clearly identified in annual SLA and SST variations. These amphidromes are located in the tropical areas of the Pacific, Atlantic and Indian Oceans. Their existence implies that the annual cycle (in time) of the atmosphere-ocean system is translated into a rotary variation (in space) for many of the geophysical parameters. It can be concluded that annual amphidromes are common, the knowledge of which is of particular interest, given their annually “constant” nature, for the monitoring and understanding of oceanic, climatic, as well as biological variabilities at seasonal to decadal scales, which strongly affect many aspects of the natural and societal activities on the globe.

1. Introduction

As a scientific term in oceanography, “amphidrome” is traditionally linked to ocean tides [1]. It normally refers to a “no-tide” point in the sea where the amplitude is zero and the phase is undetermined. About a dozen well-defined amphidromic points associated with diurnal and semidiurnal tides exist in the world ocean, forming a fundamental feature of the global tidal system.

It is well known that sea level variability can be decomposed into a number of significant components ranging from semidiurnal to inter-decadal. For the majority of the world’s oceans the leading modes in terms of intensity are definitely the semidiurnal and diurnal tides, followed by the annual mode as the secondary signal. The seasonal sea level variation may be considered to be like an annual tide in its apparent properties. This leads to the reasonable speculation that annual sea level amphidromes may exist in the global ocean. Identification of such amphidromes, however, could be a challenging task for at least two reasons. First, the annual non-tidal signal is due to changes in solar heating and wind-induced currents, whose periodicity is less stable than the tidal signals due to gravitational attraction by the sun and the moon. Second, the amplitude of the tidal signal is usually an order of magnitude larger than that of the annual signal. The combination of these two factors means that the tidal peaks in the sea level spectrum are much higher and narrower than the annual non-tidal peaks, and hence these annual amphidromes are considerably more difficult to identify due to a much lower signal to noise ratio.

However, the ability to find annual amphidromes seems to be supported by the results of previous studies based on Geosat and TOPEX altimeter data. In fact, annual phase maps have been produced and analyzed by several researchers in an attempt to characterize the seasonal change of global sea level (see Plate 1d in [2]; Figure 6 in [3]; Plate 2 in [4]; Plate 4b in [5]; Plate 1b in [6]; Plate 6b in [7]). The main conclusions concerning the annual phase pattern can be summarized as follows: 1) An autumn-spring phase dependence exists between the two hemispheres at subtropical and temperate latitudes; 2) A wind-controlled complex phase structure associated with the seasonal fluctuation of the equatorial current systems is found in the tropical oceans; 3) A phase front across the Antarctic Circumpolar Current is evident with the sea level peaks in March-April to the north, and in August-September to the south. Unfortunately, none of these investigations have addressed the amphidrome issue although it

is already partially visible in a somewhat unclear manner in some of the results. For instance, an annual amphidrome off western Australia in the Indian Ocean is identifiable in Plate 1b in [6]. This example demonstrates that there is a realistic possibility that the amphidromic system of annual sea level variation may be revealed better by satellite altimeter data of higher quality and longer duration.

2. Annual sea level amphidromes

Following the successive launch of several altimetric missions during the past two decades, the spatial/temporal resolving power in sea level measurement by the multi-altimeter system has been dramatically enhanced. Taking advantage of the recent availability of merged TOPEX/ERS/ENVISAT/JASON altimeter data spanning 1992 through 2003 [8], the annual phase characteristics of the global sea level are re-examined. The original 1/3°×1/3° weekly averaged sea level anomalies (SLA) have had all standard altimetric corrections applied [9], including a full tidal model. For our analysis these data are then smoothed using an inverse distance weighting scheme with a scanning radius of 6°, yielding 590 weekly SLA fields with a 1°×1° spatial resolution.

Figure 1(a) shows the month in which the annual SLA cycle peaks. As expected, the emerging phase pattern, though still complex in character, is much better defined compared with similar results published before. The most significant improvement is that some of the climatological features that were previously masked by short-term variability have now emerged to a large extent, thanks to the unprecedented resolution, precision, and duration of the new dataset. On a global scale, a general hemispheric phase reversal holds between two different width zonal bands: 20°-65°N in the northern hemisphere which peaks in September-October, and 25°-55°S in the southern hemisphere which peaks in March-April. The Black Sea peaks earlier (May) than the Mediterranean, because of increased riverine input to the former during the early part of the year [10]. In all the tropical oceans the phase pattern is dominated by large-scale rotating systems with clearly defined mid-ocean amphidromes, which were basically absent in previous maps of this kind. This is unlikely to be a manifestation of the annual tide, since these data have been corrected by a full tidal model, and the amplitude of long period astronomic tides is much smaller than steric departures at all latitudes [11]. For a more detailed examination of these striking structures enlarged phase

maps of the tropical Pacific, Atlantic and Indian Oceans are shown in Figures 1(b), 1(c) and 1(d), respectively.

Figures 1(a), (b), (c), and (d)

In the Pacific Ocean, the phase distribution is largely zonal with three well-separated nodal points at P1, P2, and P3, as indicated in Figure 1(b) (see also Table 1 for their locations). P1, located at 126°E, 3°N, is the only such annual amphidrome suspected prior to the analysis of satellite data. A well-distributed tide gauge network had shown that the change in annual phase is constantly opposite between north Australia and the Philippines. Several researchers have long suspected that a zero-amplitude point, which they call the "Borneo amphidrome", might exist in this region [10,12,13]; the result in Figure 1(b) provides, to our knowledge, the first direct evidence that such an amphidrome does exist. Moreover, Figure 1(b) reveals that the annual sea level rotates cyclonically around this amphidrome with a radius of nearly 20°. The rate of phase change, however, is highly asymmetric with respect to the equator: The annual sea level peak occurs from March to next January in the northern hemisphere, but only in February in the southern hemisphere. The latter coincides geographically with the western Pacific warm pool which usually varies systematically as a whole [14]. P2 and P3 are a pair of amphidromes with opposite rotations located in the central tropical Pacific. A straight line connecting these two points roughly divides the seasonality of the sea level into a boreal pattern to the east, and an austral pattern to the west. Moreover, the two regions share a common feature of tongue-shaped isolines, stretching westward and eastward, respectively, reflecting the complex influences of the equatorial current system.

The Atlantic has three amphidromes (Figure 1(c)) , one to the north of the equator and two just to the south. A model of the North Atlantic shows surface heating to give an autumnal peak to SLA variations poleward of the tropics, whereas in the equatorial band there is a subsurface signal peaking approximately six months earlier [15]. Where these two effects are of equal magnitude, the net annual cycle is close to zero (depending upon the exact lag between them). High-resolution XBT data along a regular ship route down the eastern side identify a point of little net signal at 334˚E, 14˚N [16]. Our analysis locates this amphidrome, A1, 10˚ further west than sampled by the XBT line, in close agreement with Ferry et al. [15]. This amphidrome is dramatically distorted with the northern hemisphere winter sectors

(December through next April) being shrunk to a minimal area. Nonetheless, the amphidromic nature of this point is still clear enough to be identified. The geophysical background for the extremely distorted structure, however, is difficult to explain. A2 and A3 appear as twin amphidromes in character. They share a spindle-shaped zone extending southeastward with a delayed phase in April and May. Acting as two nodes across the equatorial Atlantic, the sea level between them peaks in July, whereas that to the west of A2 and northeast of A3 are nearly 180° different in phase.

In the Indian Ocean, the annual phase distribution is characterized by the coexistence of two well-defined amphidromes, I1 and I2, of opposite rotation (Figure 1(d)). Moreover, they are connected within the rectangular area bounded by I1 and I2 (as indicated by the solid white box), sharing the co-phase lines from September to next February. It should also be noticed that the phase pattern surrounding this zone has been interpreted by several researchers as annual Rossby wave propagation. Périgaud and Delecluse [17], among others, show that off-equatorial annual sea level variations propagate westward and poleward as Rossby waves in the southern tropical Indian Ocean (STIO) north of 20°S. But a close inspection on Figure 1(d) reveals that the zone of "popular Rossby waves" identified by previous researchers (50°–120°E, 8°–20°S, as indicated by the dashed white box) coincides with a special portion of the double rotation system (see the solid white box), whose propagation properties are compatible with Rossby wave theory. It may be that Rossby waves provide the full explanation for the variation in observed sea surface height seasonality in this region. However, the longitudinally-varying phase structure could be partially due to annual variations in sea surface temperature (SST), wind and rainfall, such that some of the signal attributable to Rossby waves may correspond to other phenomena. This seems to be echoed by the controversies over their generating mechanisms. Woodberry et al. [18] and Qu et al. [19] point out that the signal is generated in the eastern Indian Ocean, east of 100°E, by the annual cycle of the wind stress curl associated with the strong monsoons. On the other hand, Périgaud and Delecluse [17] indicate that the wind stress curl at and east of the location of the maximum amplitude is weak, and that the signal propagates from the boundary. More recently, Masumoto and Meyers [20] demonstrate that the westward propagation in annual and interannual signals is mainly generated by Ekman pumping over the region. They further argue that, owing to propagation of Rossby waves, the forcing region is not localized in the eastern part of the STIO as suggested by Woodberry et al. [18]. It goes beyond the scope of

this letter to comment further on these debates, but what becomes obvious is that interpretation of sea level variation in the STIO will benefit from taking into account the entire picture of the double-amphidrome system. Also, although the annual sea level peaks coherently around the Arabian Sea and most of the Indian coast during March-April, the SLA peak is very different in the eastern Bay of Bengal. The monsoon winds are responsible for SLA in the Arabian Sea peaking much earlier than would be caused by merely steric response to solar heating. This "anomalous" forcing leads to the existence of the I1 amphidrome and the nearly 180° phase change across the Bay of Bengal.

3. Annual SST amphidromes

Following the successful identification of annual amphidromes in sea level variation, we were inspired to examine similar features in another oceanic parameter. Sea surface temperature (SST) was selected for this purpose since it is one of the most useful variables in oceanographic and meteorological studies. The SST data are extracted from a NOAA/NASA Oceans Pathfinder Product called "Equal Angle Best SST", which has resolutions of 9 km and 7 days [21]. The data were interpolated to a 1°×1° spatial grid and a 1-month time interval.

The annual phase map of SST is shown in Figure 2. As expected, the phase distribution is basically hemispherically divided. The majority of North (South) Pacific and North (South) Atlantic have their SST peaks in August-September (February-March). The Indian Ocean largely follows a southern hemisphere pattern in SST variation, except for the Arabian Sea and Bay of Bengal, which appear to have an intermediate seasonality with respect to the two hemispheres. The SSTs of these areas are strongly controlled by the seasonal monsoon through breakdown of stratification and enhanced mixing, as well as through the shift of surface flow. Focusing on the equatorial areas of the Pacific and Atlantic Oceans, one finds that two annual amphidromes are clearly evident at T1 and T2, respectively (Figure 2, see also Table 1). The phase rotation is cyclonic around both, with the change of phase highly asymmetric in space and very high gradients occurring within 10°S-10°N during April-October.

Figure 2

4. Discussions

The direct effect of changes in insolation explains most of the seasonality observed in SST. For most mid and high latitude locations, the peak in SLA follows about a month later, as the steric contribution to the height signal integrates the effect of the heating over the upper mixed layer. However, the complexity of the pattern in Figure 1 shows that other effects, such as wind-induced buoyancy forcing, also have an impact on the SLA seasonal cycle. Consequently the SLA amphidromes would not be expected to coincide with SST ones. The earlier peak in SLA around 10-15˚N in the Pacific may be due to Ekman pumping [22]. Seasonal SLA variations in the central belt of the Atlantic are governed by sub-surface buoyancy forcing, whereas north of that changes are due to heating of the surface layer [15,16]. Where these effects are of equal amplitude and exactly opposite phase, there is no net seasonal signal. This produces the well-determined A1 amphidrome, which was apparent in earlier analyses [7,15]. Translating the argument to the Pacific and Indian basins, one would expect SLA amphidromes to lie on the edge of sub-surface seasonally-modified waters. In the Pacific this band would be equatorial, but in the Indian Ocean it may correspond to the broad Southern Equatorial Current, straddled by I1 and I2. Stammer [7] had found the seasonal cycle to the south of 50˚S to peak six months earlier than the waters at 40˚S; our analysis of a larger dataset shows a less clear zonal signal, with the mean advancement being only three months.

Although there is little doubt about the existence of annual amphidromes in the ocean given their well-defined spatial structures, the stability of these zero-amplitude points is certainly something to be further examined. To do so, the SLA data were divided into two subsets of equal duration, and annual phase maps generated for each (not shown). The locations of the eight annual amphidromes in SLA remain almost unchanged (within 1°–2°), whereas for SST, a 2°–5° zonal shift is observed between the first and second halves of the data (not shown). These changes are found to be most significant in the Pacific Ocean while least so in the Atlantic Ocean, which is likely to be a reflection of the El Niño–Southern Oscillation effect. They may also be a manifestation of decadal or even longer-period oceanographic/meteorological variations. But in both cases, the general patterns of the phase distributions are very consistent between the two periods. It can therefore be concluded that the identified annual amphidromes associated with oceanic parameters are stable in a climatological sense.

5. Summary and concluding remarks

To summarize, more than a decade of high quality satellite observations have allowed eight annual amphidromes to be clearly revealed for sea level, and two for sea surface temperature. Among them the Borneo amphidrome, which is the only one that has been explicitly mentioned before, is convincingly confirmed by our result. The new findings on the amphidromic structure of annual sea level variation may be helpful in interpreting and understanding some of the propagation patterns associated with subtropical Rossby waves. The SST amphidromes around which the temperature has no seasonal variation are likely to be of importance for some of the biological and fishery processes in the equatorial Pacific and Atlantic. The observed complexity of annual sea level and SST variations, particularly their phase patterns, is a combined result of meteorological and oceanographic forcings, gravitational and hydrological contributions, as well as geographic and topographic effects. Among them, the boundary effect, i.e., the land-ocean distribution as well as the bottom topography, is likely to be a fundamental factor. If the earth were completely covered by a homogeneous ocean, the phase pattern would be basically zonal. The latitudinal progression of the oceanic season is significantly influenced and altered by the 3-D asymmetric distribution of the landmass along with other effects. The dominant factor for each amphidrome, however, may vary from basin to basin, and from latitude to latitude.

Identification of the annual sea level and SST amphidromes, and potentially many others associated with various geophysical parameters, has a number of direct and/or indirect implications. Most obviously, these open ocean amphidromic points could be the ideal sites for monitoring interannual to decadal sea level change and global warming, since they are, in theory, free from interference of energetic seasonal signals. Also, understanding of the annual amphidromic structure, especially its asymmetric pattern is useful in guiding future deployment of gauges and buoys for a more effective and efficient observation of global and regional sea level changes. In addition, knowledge of the annual amphidromic system may also be of potential importance to some of the dynamical processes such as Rossby wave propagation in the ocean.

Acknowledgements

NASA, NOAA, ESA, CNES and CLS are gratefully acknowledged for making the satellite data available. The authors thank Drs. Meric Srokosz and Michael Tsimplis for their helpful comments on an earlier version of this paper. This research is jointly supported by the Natural Science Foundation of China (Project No.: 40025615) and the Royal Society of the UK.

References

[1] T. Garrison, "Oceanography: An Invitation to Marine Science", Wadsworth Pub. Co., Belmont, 567pp., 1996.

[2] G. A. Jacobs, G. H. Born, M. E. Parke, and P. C. Allen, "The global structure of the annual and semiannual sea surface height variability from Geosat altimeter data". *J. Geophys. Res.*, vol. 97, no. C11, pp. 17813-17828, Nov. 1992.

[3] R. Cheney, L. Miller, R. Agreen, and N. Doyle, "TOPEX/POSEIDON: The 2-cm solution". *J. Geophys. Res.*, vol. 99, no. C12, pp. 24555-24563, Dec. 1994.

[4] R. S. Nerem, E. J. Schrama, C. J. Koblinsky, and B. D. Beckley, "A preliminary evaluation of ocean topography from the TOPEX/POSEIDON mission". *J. Geophys. Res.*, vol. 99, no. C12, pp. 24565-24583, Dec. 1994.

[5] D. Stammer, and C. Wunsch, "Preliminary assessment of the accuracy and precision of TOPEX/POSEIDON altimeter data with respect to the large-scale ocean circulation". *J. Geophys. Res.*, vol. 99, no. C12, pp. 24584-24604, Dec. 1994.

[6] P. Knudsen, "Global low harmonic degree models of the seasonal variability and residual ocean tides from TOPEX/POSEIDON altimeter data". *J. Geophys. Res.*, vol. 99, no. C12, pp. 24643-24655, Dec. 1994.

[7] D. Stammer, "Steric and wind-induced changes in TOPEX/POSEIDON large-scale sea surface topography observations". *J. Geophys. Res.*, vol. 102, no. C9, pp. 20987-21009, Sept. 1997.

[8] CLS, "SSALTO/DUACS User Handbook, (M)SLA and (M)ADT Near Real Time and Delayed Time Products", CLS-DOS-NT-04.103, Version 1 rev. 3, Ramonville, France, 51pp., 2004.

[9] P.-Y. .LeTraon, F. Nadal, and N. Ducet, "An improved mapping method of multisatellite altimeter data". *J. Atmos. Oceanic Tech.*, vol. 15, no. 2, pp. 522-534, Apr. 1998.

[10] M. N. Tsimplis, and P. L. Woodworth, "The global distribution of the seasonal sea level cycle calculated from coastal tide gauge data". *J. Geophys. Res.*, vol. 99, no. C8, pp.

16031-16039, Aug. 1994.

[11] J. Pattulo, W. Munk, R. Revelle, and E. Stong, "The seasonal oscillation in sea level". *J. Mar. Res.*, vol. 14, no, 1, pp. 88-113, 1955.

[12] E. Lisitzin, "Sea-Level Changes", *Elsevier Oceanogr. Ser.*, vol. 8, 286 pp., Elsevier, New York, 1974.

[13] P. L. Woodworth, "The worldwide distribution of the seasonal cycle of mean sea level", *Rep. 190,* 94 pp., Inst. of Oceanogr. Sci., Bidston Observ., Birdenhead, England, 1984.

[14] G. Chen, C. Fang, C. Zhang, and Y. Chen, "Observing the coupling effect between warm pool and “rain pool” in the tropical Pacific". *Remote Sens. Environ.*, vol. 91, no. 2, pp. 153-159, May 2004.

[15] N. Ferry, G. Reverdin, and A. Oschlies, "Seasonal sea surface height variability in the North Atlantic Ocean", *J. Geophys. Res*. vol. 105, no. C3, pp. 6307-6326, Mar. 2000.

[16] D. A. Mayer, R. L. Molinari, M. O. Baringer, and G. J Goni, "Transition regions and their role in the relationship between sea surface height and subsurface temperature structure in the Atlantic Ocean" , *Geophys. Res. Lett.* vol. 28, no. 20, pp. 3943-3946, Oct. 2001.

[17] C. Périgaud, and P. Delecluse, "Annual sea level variations in the southern tropical Indian Ocean from Geosat and shallow-water simulations". *J. Geophys. Res.*, vol. 97, no. C12, pp. 20169-20178, Dec. 1992.

[18] K. E. Woodberry, M. E. Luther, and J. J. O’Brien, "The wind-driven seasonal circulation in the southern tropical Indian Ocean". *J. Geophys. Res.*, vol. 94, no. C12, pp. 17985-18002, Dec. 1989.

[19] T. Qu, G. Meyers, J. S. Godfrey, and D. Hu, "Ocean dynamics in the region between Australia and Indonesia and its influence on the variation of the sea surface temperature in a global general circulation model". *J. Geophys. Res.*, vol. 99, no. C9, pp. 18433-18445, Sept. 1994.

[20] Y. Masumoto, and G. Meyers, "Forced Rossby waves in the southern tropical Indian Ocean". *J. Geophys. Res.*, vol. 103, no. C12, pp. 27589-27602, Nov. 1998.

[21] J. Vazquez, K. Perry, and K. Kilpatrick, *NOAA/NASA AVHRR Oceans Pathfinder sea surface temperature data set user's reference manual*, Version 4.0. JPL Publication D-14070, 1998.

[22] F. Vivier, K. A. Kelly, and L. A. Thompson, "Contribution of wind forcing, waves and surface heating to sea surface height observations in the Pacific Ocean. *J. Geophys. Res.*, vol. 104, no. C9, pp. 27589-27602, Sept. 1999.

Table 1. Locations of the annual sea level and SST amphidromes in the global ocean.

Ocean	Amphidrome	Location
Pacific Ocean	P1	(126°E, 3°N)
	P2	(178°E, 7°N)
	P3	(225°E, 14°S)
	T1	(189°E, 4°S)
Atlantic Ocean	A1	(325°E, 13°N)
	A2	(332°E, 9°S)
	A3	(339°E, 6°S)
	T2	(336°E, 5°N)
Indian Ocean	I1	(55°E, 5°S)
	I2	(104°E, 27°S)

Figure Captions

Figure 1. (a) Map of the month when fitted annual SLA cycle peaks. [Data are from a merged TOPEX/ERS/ENVISAT/JASON altimeter dataset spanning 1992 though 2003.] (b), (c) and (d) are enlarged maps of tropical regions of Pacific, Atlantic, and Indian Oceans, respectively. Positions of annual SLA amphidromes are marked by white circles.

Figure 2. Map of the month when fitted annual SST cycle peaks. [Data are from a NOAA AVHRR dataset spanning 1985 though 2003.]

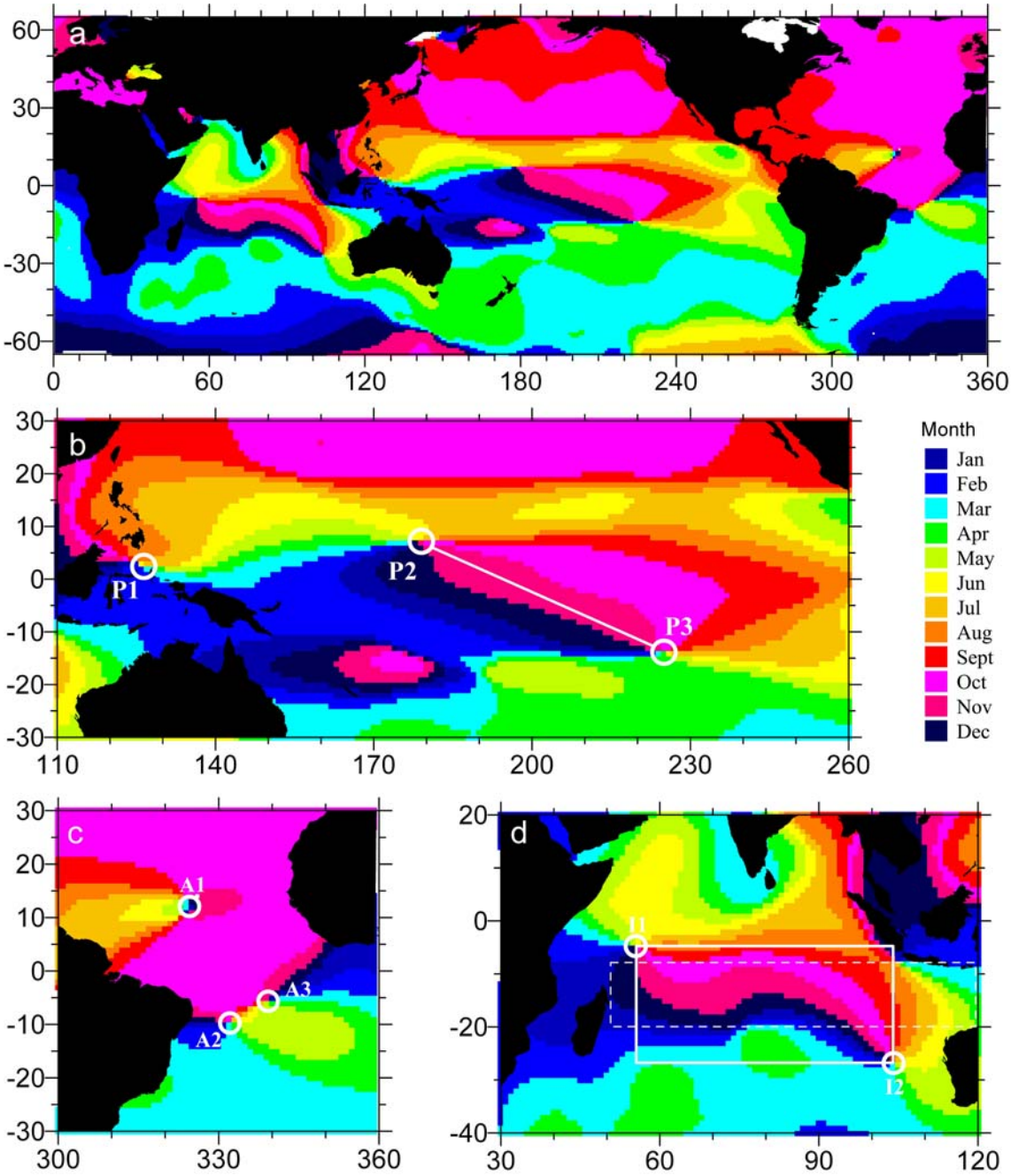

Figure 1. (a) Map of the month when fitted annual SLA cycle peaks. [Data are from a merged TOPEX/ERS/ENVISAT/JASON altimeter dataset spanning 1992 though 2003.] (b), (c) and (d) are enlarged maps of tropical regions of Pacific, Atlantic, and Indian Oceans, respectively. Positions of annual SLA amphidromes are marked by white circles.

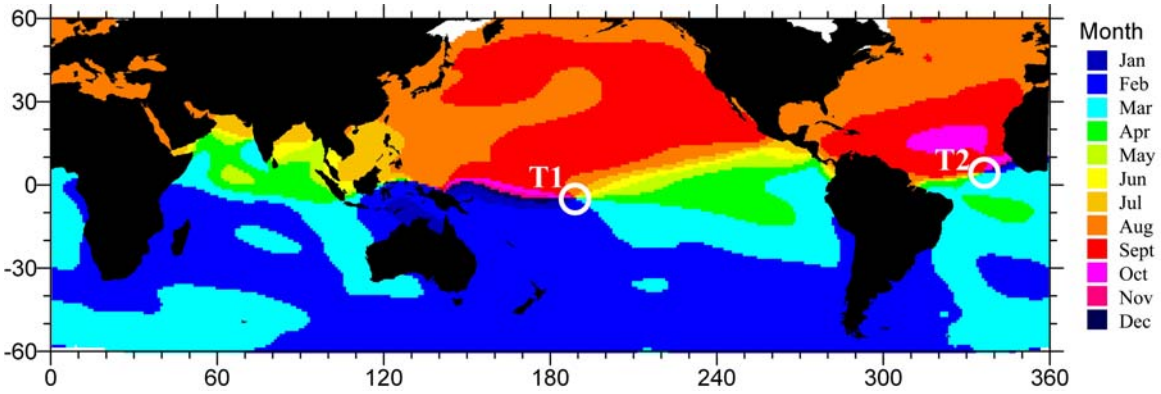

Figure 2. Map of the month when fitted annual SST cycle peaks. [Data are from a NOAA AVHRR dataset spanning 1985 though 2003.]